Photophysical and Photodecomposition Studies on Polyethylenes: A Novel Application of Gas-Phase Mirage-Effect Spectroscopy

B. L. ZIMMERING,[1] AJAY KUMAR,[2] A. C. BOCCARA,[1] G. C. PANDEY[2]

[1] Laboratoire de Optique Physique, E.S.P.C.I., 10 rue Vauquelin, 75005 Paris, France

[2] Research Center, Indian Petrochemicals Corporation Ltd., Baroda-391346, India

Received 12 June 1997; accepted 5 October 1997

ABSTRACT: The advantage of a high signal-to-input power and path-length ratio, while retaining very good flexibility of the operation, has made the recently developed gas-phase mirage-effect spectroscopy setup an excellent tool for the measurement of trace gases and organic volatiles up to ppb or lower concentration levels. The present study demonstrates an unusual application of this novel technique in the area of the nondestructive characterization and photodecomposition of polymers. Very small quantities of ethylene gas were found to be released when polyethylenes were exposed to a very low power mercury lamp (photoexposure). The extent (quantity) of the ethylene gas produced was found to be specific and characteristic of the type of polyethylenes (e.g., HDPE and LDPE). The source of ethylene was attributed to the rupture of the terminal monomer units of the branched chains. This study, apart from fundamental understanding, also demonstrated a direct industrial application in the fast and nondestructive characterization of various polyethylenes. © 1998 John Wiley & Sons, Inc. J Appl Polym Sci 69: 1875–1883, 1998

Key words: polymers; polyethylenes; photodecomposition; gas phase; mirage effect; photothermal; spectroscopy

INTRODUCTION

Polyolefins (PO) form one of the most important thermoplastics in the world in view of their wide range of applications from day-to-day use in the domestic sector to highly sophisticated and hi-tech industrial sectors such as aviation. Such a wide range of applications, in turn, calls for an equally important aspect, that is, a detailed study on the wide spectrum of their evaluation to ensure reliability and product quality under different environmental conditions. Degradation or decomposition is one such characteristic property which has been used as a measure of product quality. The most common type of degradation occurs through chemical reactions (e.g., chain reaction, crosslinking, side-group elimination, or chemical-structure modification, alone or in combination), although those leading to physical changes (e.g., description of polymer morphology or of secondary bonds on macromolecule conformational changes) have also been reported. Vasile[1] reported a list of degradation agents and types of degradation. In general, an understanding of the physical and chemical degradation processes and that of the products formed has an important impact on the development of practical applications. It may be worth pointing out here that processes involving

Correspondence to: G. C. Pandey.

Contract grant sponsor: Indo-French Centre for Advance Research, New Delhi.

Journal of Applied Polymer Science, Vol. 69, 1875–1883 (1998)
© 1998 John Wiley & Sons, Inc. CCC 0021-8995/98/091875-09

light (UV/vis) are termed as photochemical degradation, and those involving light and oxygen, as photooxidation, and heat and oxygen, as thermooxidative degradation and/or decomposition/combustion.

In the light of the above, the present work may be classified in the category of photodegradation, while the majority of the reported literature in this domain concerns mainly thermooxidative degradation. Thermal oxidation includes migration, propagation, chain branching, and termination steps and is polymer-specific. For instance, chain scission is characteristic of polypropylene, whereas simultaneous chain scission/chain branching leads to the crosslinking characteristic of polyethylene (PE).

A detailed survey of more than 30 years of the literature has shown that virtually no work has been reported on the gaseous products formed as a result of the photodecomposition of PEs, although considerable references are available on the effect on polymer substrates.[2–4] In an effort to obtain information on the gaseous products formed as a result of the photochemical decomposition of polymers with special reference to PE, a detailed study was undertaken on the use of a novel gas detection technique called photothermal beam deflection spectroscopy (PTBDS, also called mirage-effect spectroscopy) which permits real-time multiple species detection on a sub-ppb level. The capabilities of a sensor[5] founded on this technique make its use well suited to the measurement of gases produced during PE photodegradation. A similar detection system has been used to evaluate the detrimental effects of gas produced by PE tubing in response to fluorescent light sources and has shown that gas quantities can be sufficient to interfere with high-precision gas-phase measurements.[6] In this work, we propose to use the measurement of these gas-phase effluents as an analytical tool to study the photochemical reactions of PEs. The results will allow us to propose an interpretation from a mechanistic standpoint.

Gas-Phase PTBD or Mirage-Effect Spectroscopy: Principle

Photothermal spectroscopic (notably photoacoustic, thermal lens, and mirage detection) methods offer many advantages applicable to trace gas detection, including high sensitivity and signal reference to a true zero. Gas-phase photoacoustic (PA) studies use a microphone to measure the expansion of a sample heated by laser absorption and have been successfully used by several researchers for trace gas detection into the ppb and several tenth ppt (when intracavity detection is used) range.[7–12] The limitations imposed by use of an enclosed cell, usually necessary for optimal performance, reduce the flexibility of the system, imply window transmission losses, and finite volume sampling and pumping of the gas into the cell. This makes real-time *in situ* measurements difficult to perform, and, in addition, susceptibility of the system to gas entrapment by the microphone place limits on the choice of the subject gas to be studied. Furthermore, temperature stability requirements may exclude use in some industrial or other applications in "noisy" environments. The use of photothermal deflection or mirage-effect spectroscopy for trace gas detection has demonstrated roughly the same order of sensitivity as that of PA spectroscopy, but with many advantages for use in practical settings because of improved flexibility.[13–15]

As in classical absorption spectroscopy, the sample to be studied by PTBDS is heated by absorption of a modulated (pump) laser source. The thermal gradient induces a time-dependent refractive index gradient within the heated region. A second (probe) laser beam, passing through the heated region, is deflected through an angle directly related to the local thermal gradient (Fig. 1). We show in this figure the "collinear" geometry which we use in our experiment; the pump and probe beams are aligned parallel to one another, and the much smaller dimension of the probe beam allows its shape to be neglected (treated as a line of zero diameter). The thermal gradient therefore produces an effect upon the probe comparable to a lens. The induced deflection is measured with a photodiode pair position detector. The parameters which contribute to the signal depend on the relative magnitudes of the thermal diffusion length $\mu = \sqrt{2k/\rho c\omega}$ and the pump beam waist. In the case where the thermal diffusion length is much larger, due to a high modulation frequency, or where the medium has a low thermal diffusivity, the deflection angle is given by

$$\phi = -2\left(\frac{x_0}{a^2}\right)\left(\frac{dn}{dT}\right)\frac{P}{\omega\rho c\pi^2 a^2} \times [1 - \exp(-al)]\exp\left(\frac{-x_0^2}{a^2}\right)$$

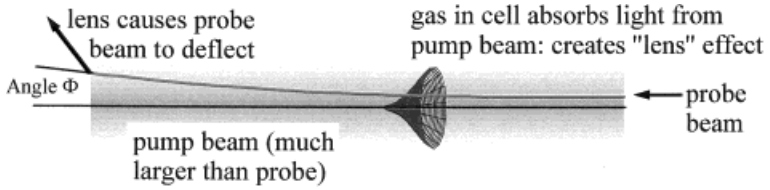

Figure 1 Principle of PTBDS.

where dn/dT is the temperature coefficient of the index of refraction of the gas; P, the incident laser power; ω, the laser modulation frequency; ρc, the thermal heat capacity; α, the concentration-corrected optical absorption coefficient; l, the interaction path length; a, the pump beam radius, and x_0, the separation between the pump and probe beams. We note that when this separation distance is approximately equal to the pump beam diameter the signal is at a maximum, and so the position adjustment of at least one beam is desirable to optimize performance. We performed all measurements within the high-frequency condition, because of the particular power stability characteristics of our pump laser and the smaller noise level in open-air measurement.

In a gas-phase medium, the laser power absorbed is linearly proportional to the concentration of the absorbing gas species up to the saturation limit. We can see that in the above equation, for small al, the corresponding deflection signal is also approximately linear with the gas concentration. In addition, as the measured signal is generated in proportion to the absorbed energy, the sensitivity may approach the shot noise limit. This technique is extended to selection between multiple gas species in a mixture by the use of a tunable pump laser. A frequency resonant with a vibrational mode of the species to be detected is chosen, taking care to avoid resonance with other molecules in the mixture. This gas species alone then absorbs the excitation, and the mixture is heated through kinetic quenching. Detection thus has species selectivity equivalent to that of direct absorption spectroscopy with much higher sensitivity for the same quantity of the absorbed energy.

Description of the Instrument

Our experimental setup is shown in Figure 2. The CO_2 pump laser used is commercially available* and uses a single plasma tube grating tunable configuration with over 60 available lines and a TEM_{00} mode adjustment due to an adjustment of the off-axis grating tilt. The modulation depth is 100% at 135 Hz, with a typical output power of 1–3 W. This grating tunable laser allows the detection and differentiation of many gas species important to environmental surveillance such as COT/COV (including volatiles), NH_3, SO_2, O_3, H_2S, and NO_2 owing to the large number of available laser lines. A selection of available gases for environmental applications is listed in Table I. The ZnSe focusing lens is mounted with micrometric position adjustments for optimization of the relative parallel displacement between the pump and probe beams. The aluminum detection cell is fitted with 1.5-mm-thick germanium (Ge) windows set at the Brewster angle at 10 μm for the CO_2 laser polarization. The transmission losses in the windows are thus minimal. The Ge windows serve as beam splitters, which while transmitting the CO_2 beam reflect and orient the probe beam, produced by a 1.5-mW HeNe laser located below the detection cell. The HeNe focusing mirror is mounted with a micrometric position adjustment along the beam propagation direction and spring-loaded screws to enable both position and parallelism adjustment by manipulation of the slew and tilt angles.

The HeNe beam is rereflected by the exit Ge window onto the photodiode position detector. The photodiode signal is measured by lock-in detection using the laser modulation control signal as the frequency reference, with a time constant of 0.3 s. The detector is located 15 cm from the interaction region. The interaction length in the cell is 20 cm, and the cell interior volume is 25 mL. The interior may be exposed to open air by removal of a plate on the top of the cell. The gas-handling system for the manipulation of the calibrated mixtures uses

* SYNRAD Model 48-G-1 with UC-1000 controller.

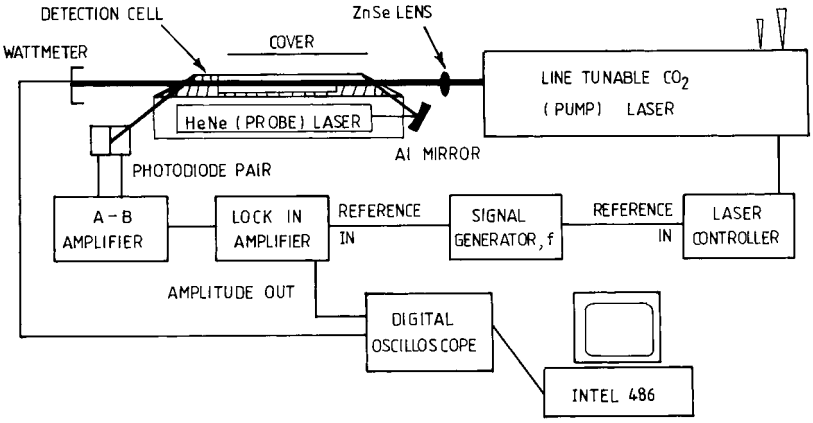

Figure 2 Experimental setup.

stainless-steel Hoke fittings and tubing, to avoid parasite signals due to gas which could be produced by plastic tubing.

Measurement Method

For typical gas-detection applications, the signal is continuously measured while the laser line (wavelength) is varied, allowing measurement of the sample's spectral characteristics and their variation in time. A linear analysis allows interpretation of this signal in order to identify the gas species present and their respective concentrations. In this study, polymer films are placed inside the detection cell and illuminated by a low-pressure Hg lamp fixed atop a cell cover with silica windows. The UV light initiates the photochemical reactions in the films, resulting in the production of hydrocarbon gas. These gases are accumulated in the cell and we measure the time evolution of the signal on five CO_2 laser lines (P, J = 10P10-18).

Table I Detection Limits of Some of the Organic Volatile Compounds Measured by the Gas-Phase Mirage Setup

Gas	Detection Limit (ppb)
C_2H_4 (ethylene)	0.25
C_2Cl_3H (trichlorethylene)	2.5
C_6H_6 (benzene)	12
C_8H_{10} (xylene)	20
CFC-11/Freon-11	0.6
C_2H_3Cl (vinyl chloride)	45
SO_2	240
NO_2	10
NH_3	0.5
O_3	2.5

Mechanism of Photodecomposition of Polyolefins (POs)

Exposure of POs in general and polyethylenes (PE) in particular to electromagnetic radiation (UV-vis) has been an important area of research as is evident from a large number of articles reported in the literature dealing with fundamental aspects like kinetics and photodegradation mechanisms. In principle, natural sunlight is not expected to have any effect on C—C and C—H bonds (basic constituent units of POs) as they absorb radiation of $\lambda < 190$ nm while most of the studies reported use $\lambda > 300$ nm. Thus, initiation of photodegradation of such systems is possible only through absorption of photons by an impurity in the polymers or by chromophoric groups. Because of the complexities involved during different stages of polymerization, posttreatments like processing or addition of stabilizers and/or antioxidants, it is nearly impossible to pinpoint the real cause of oxidation in PEs; however. Gugamus carried out an extensive study on photodecomposition of PEs detailed in a series of articles.[16–23] He concluded that the photolysis of free hydroperoxides which had been generated thermally proceeds according to a mechanism which does not involve intermediate formation of free radicals.[18–20] He further suggested the formation of PE and an oxygen ($P\cdots O_2$) charge-transfer complex (CTC) by way of photooxidation of PE which, in turn, acts as an initiator, leading to the formation of a *trans*-vinyl group and hydrogen peroxide.[17,19] The latter, upon absorption of a UV pho-

ton, changes into a hydroxyl radical and initiates PE oxidation through hydrogen abstraction. This literature has also shown that depending upon the type of polymer and its constituents a variety of radical reactions are possible.[18,20,23] For instance, recombination of two radicals (R′—R) leads to increased molecular weight[1] and the addition radical —C=C— is energetically favored by the formation of a σ bond at the expense of a π bond[24]:

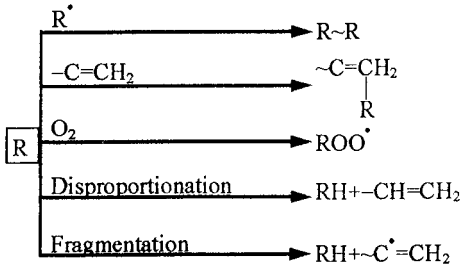

RESULTS AND DISCUSSION

The available data on photooxidation of polyolefins leads one to conclude that the mechanism of reaction is not very well understood. Free-radical (polymer) chain oxidation initiated by the photolysis of hydroperoxide has been suggested to be the most important route and is used as an explanation in most of the reported literature. In the early 1990s, much interest was generated concerning PE degradation as evidenced by several articles during this period.

Gugamus recently reported an extensive study on PE and suggested that the photolysis of free hydroperoxide, which has been generated thermally, proceeds according to various routes not involving intermediate formation of free radicals.[19–21] He considered the PE–oxygen CTC as the primary initiating species upon photooxidation of PE,[20] which, in turn, yields a *trans*-vinylene group and hydroperoxide. The latter is converted into a hydroxy radical through hydrogen abstraction.[16–20] After peroxidation, this pair usually undergoes a bimolecular reaction, which, in the case of PE, leads to the formation of mainly ketones and secondary alcohols.[20] This mechanism explains most of the observations and also the formation of chromophores (e.g., ketones, aldehydes, and hydroxides) through the initial oxidation, which normally act as photon absorbers (sinks), leading to further degradation of thermally initiated oxidation of the polymer. It may be pointed out that in most of the reported studies the thermal (infrared region) part of the source radiation seems to be the source of the thermal energy considered for initiation of the reaction.

The present work, on the other hand, was undertaken with a view to exclude the possibility of thermal energy during photoexposure of the PE. This was achieved by using a very low power exposure source effective power $\approx$ 0.25 W for short durations. In the absence of any relevant information in the reported literature on the major gaseous products produced and also the effect on the polymer formation itself (e.g., formation of C=O) as a result of photoexposure, a detailed study was carried out with a view to

1. identify the major components of the gaseous products and the mechanistic aspect of photodegradation and
2. explore possible industrial application of the present study, for instance, characterization of PEs or monomer recovery from wastes.

No oxidation of PE was observed based on the absence of any bands in the infrared (IR) spectrum, characteristic of oxidized PE. In fact, a digital comparison of the IR spectra of PEs before and after photoexposure indicated a close similarity between the two (Fig. 3). This was also confirmed from the fact that there was no observable morphological change in the PE after the exposure.

Spectral analysis of the gaseous products formed indicated ethylene to be the dominant component. This was confirmed by comparison of the spectral signature of these products to that of pure ethylene. Figure 4 shows these spectra with 1 ppm ethylene gas (reference) and that of the (photoexposed) gaseous product. Formation of ethylene has been reported on by the thermal oxidation of PE.[24–29] Thermal oxidation is known to produce 90% water, a few percent of CO + CO_2, ethylene, and oxidized volatile organic components like acetaldehyde, acetone, butyraldehyde, 2-butane, and others in very small quantities.[25]

Our preliminary studies on two PEs, namely, low-density polyethylene (LDPE) and linear low-density polyethylene (LLDPE), indicated that ethylene gas was released during photoexposure in variable quantities depending upon the sample. This led us to extend the work to quantitative evaluation of ethylene gas by different PEs which are known to have different characteristic physicomechanical properties. The various PEs studied are tabulated in Table II. The results indicate the following pattern in terms of ethylene content:

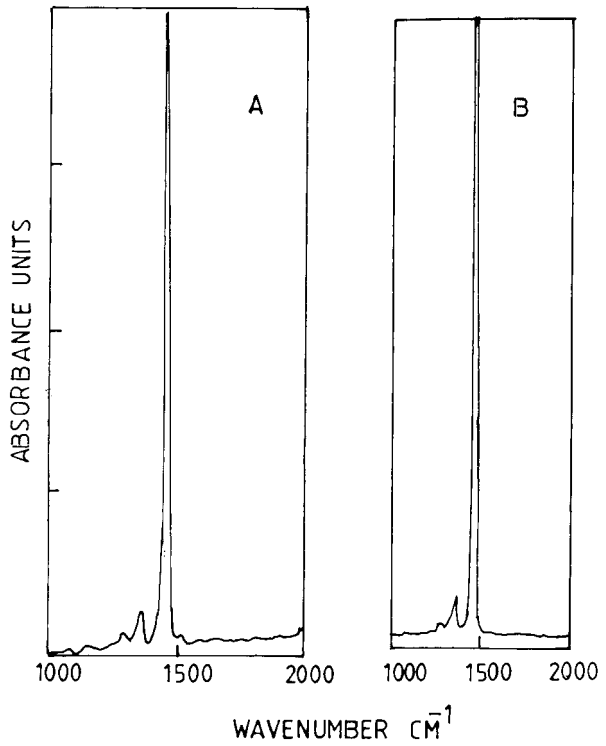

Figure 3 IR spectra of polyethylene (LDPEA) (A) before and (B) after photoexposure experiment.

$$\text{LDPE}_T > \text{LDPE}_A \gg \text{C8} \geq \text{C4} > \text{HDPE} \quad (1)$$

Further analysis of the data on these polyethylenes indicated that although the general trend was as above, the quantity of the ethylene gas (released) was considerably larger in the case of LDPEs compared to LLDPEs or HDPE. The pattern thus can be regrouped as follows:

$$\text{LDPE}_T > \text{LDPE}_A \quad (2)$$

$$\text{LLDPE C8} \geq \text{LLDPE C4} \quad (3)$$

$$\text{HDPE (very low or negligible)} \quad (4)$$

In view of the fact that the above PEs have different physicomechanical and structural properties, an attempt was made to explain the above-observed behavior based on structural properties. It may be worth mentioning here that although all the PEs are known to consist of long methylene chains, depending upon their molecular weight, the structural arrangement of these basic units are responsible for the variation in their physicomechanical properties and is the same (basis) which we hope to establish in the present work.

The high-density homopolymer (HDPE) is known to have the highest density and crystallinity of the samples studied in addition to having a basic main-chain structural arrangement. HDPE also contains the smallest number of terminal vinyledene groups. These properties, as expected, support the observation that the breaking of any of the constituent bonds will be most difficult as reflected by the amount of ethylene produced. The release of an almost negligible quantity of ethylene by the HDPE also supports these hypotheses. Other polymers in the series have relatively low density and contain alkyl substituents with branches formed during the synthesis. The LDPE resins studied were samples from two different processes and are categorized accordingly as LDPE (tubular or T) and LDPE (autoclave or A). Each has their characteristic properties which decide their ultimate applications as has been briefly mentioned in the literature by Pandey and others.[30–34] For instance, LDPE(A) has a better processability in extrusion coating than has LDPE(T) and has a long chain, treelike branching and broad bimodal molecular weight distribution. LDPE(T), on the other hand, is employed as a high-clarity film-grade resin with a linear molecular shape, broad bimodal molecular weight distribution, and high tensile strength.

A comparison of various structural features and performance features of the two LDPEs is shown in Figure 5. Analysis of the above results based on these features [eq. (2)] indicates that the long (side)-chain branching is responsible for

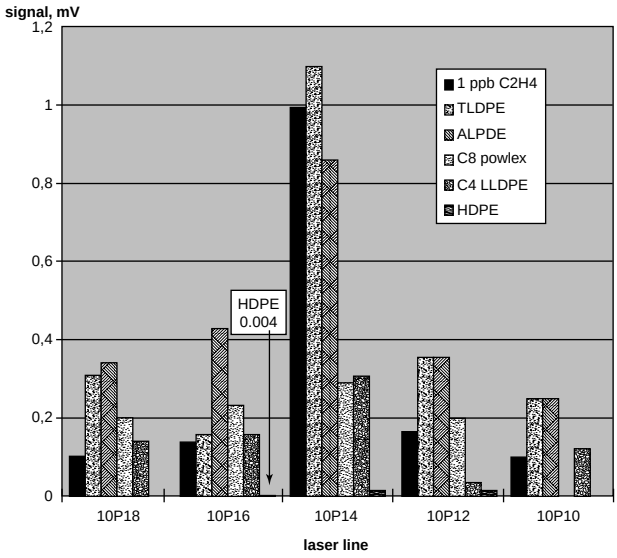

Figure 4 C2H4 reference and sample spectra.

Table II Physicomechanical Properties of Different Polyethylenes

Sample/Properties	HDPE	LDPE(T)	LDPE(A)	LLDPE C4	LLDPE C8
Density (g/cm^3)	0.962–0.968	0.917–0.936	0.914–0.930	0.919–0.924	0.918–0.924
No. methyl groups (1000)	2–3	~ 39	~ 35	—	—
Type of branching	None	LCB	LCB	SCB	SCB
No. vinylidene groups/1000	Negligible	0.47	0.84	—	—
Tensile strength (MPa)	25–45	20–22	20–22	30–45	30–38

LCB, long-chain branching; SCB, short-chain branching. Tensile strength data taken from refs. 22 and 40.

the relatively very high amount of ethylene released. This is due mainly to the easy availability of the terminal double bond of the long-chain alkyl (methyl) group, as these groups are the least influenced by the strong main chain of the PEs. This explanation is further supported by the treelike structural arrangement/features of the branched chain in LDPE(A). In turn, this is expected to be more influenced by the main chain and also by the hindered stereochemical factors responsible for the lesser quantity of the ethylene gas in the autoclave compared to tubular PE. A semiquantitative correlation between the amount of ethylene produced and that of vinylene groups per thousand carbons also supports the influence of a steric factor,[35] that is, in spite of the fact that the number of vinylene per thousand carbons (0.84) in LDPE(A) are nearly double that of LDPE(T) but both have nearly an equal number of methyl per thousand carbons (e.g., 35 and 39, respectively, Table I). These factors have also been indicated by IR spectroscopic studies on the two PEs.[30]

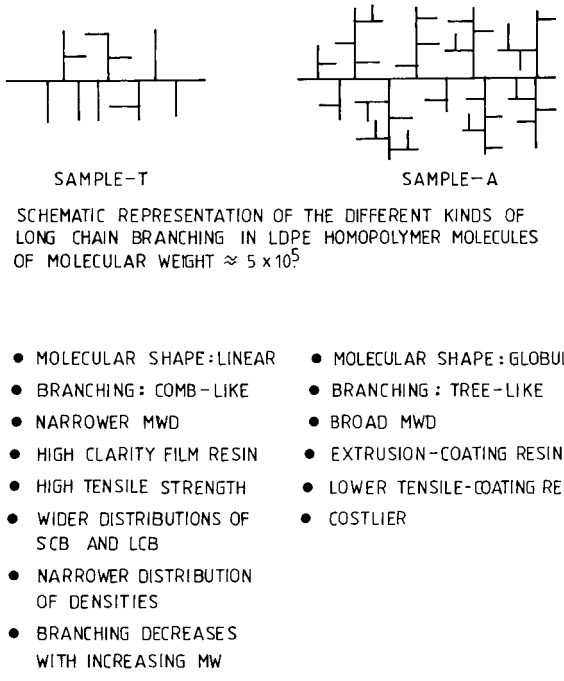

Figure 5 Schematics of structural difference between LDPE(T) and LDPE(A).

Linear two-density polyethylenes (LLDPEs) are known to include α-olefin copolymers having densities in between HDPE and LDPE. These are usually 1-butene, 1-hexene, or 1-octene. Incorporation of these comonomers in the main-chain LDPE are known to give a side chain depending upon the comonomer's chain length[36–39]:

$$\underset{\text{PE}}{\text{C—C—(C—C)}_n} + \underset{\alpha\text{-olefin}}{\text{C=C—(C—C)}_x} \rightarrow \begin{array}{l} \text{(C—} \qquad \text{C)}_x \\ \quad\ \ | \\ \text{C —C—(C—C)}_n \end{array}$$

One thus expects short-chain branches (SCBs) in the LLDPEs used for different applications. Incorporation of these comonomers leads to SCBs: The influence of the main chain onto the terminal double bond is expected to be much higher than in the long-chain branch PEs (e.g., LDPEs). The extent of the influence of this factor will be dependent upon the length of the SCBs, that is, an ethyl branch (C4) is expected to be much more strongly influenced or attached to the main-chain than will a hexyl (C8) branch. This makes terminal double bonds in a C8 copolymer relatively more labile compared to those in a C4 copolymer. In other words, structurally, C8 LLDPE may be expected to release more ethylene than does C4 LLDPE, and this is confirmed in the present work. It may be pointed out here that due to the SCBs, the influence is quite significant in both cases (C4 or C8), consistent with the observations that the ethylene quantity released by the two monomers were similar and much lower compared to long-chain branched LDPE.

Mechanism

As already mentioned, the present work ensured that no chromophores were generated on the polymer which act as photon absorbers, causing further oxidative degradation. Photons needed, therefore, a suitable (energy-deficient) site in the polymer chain for any reaction to proceed and also vinylene.

This proceeds structurally on one of the chain ends in a given PE molecule by a methyl group, that is,

$$-\!-\!CH_2\!-\!CH_2\!-\!CH_3 \qquad (6)$$

The other chain end is either a similar saturated group or it contains a double bond, typically

$$\text{Vinylidene } -\!CH_2\!=\!C\!\begin{matrix}H\\ /\\ \backslash\end{matrix} \qquad (7)$$

$$\text{or } \textit{trans}\text{-vinylidene } -\!CH\!=\!CH\!- \qquad (8)$$

Thus, the probability of a photon being absorbed at the β-carbon seems to be the most likely; this is, in turn, expected to produce ethylene as the major product of photoexposure as shown below:

$$PE \xrightarrow{h\nu} PE^* \rightarrow R(R'CH\!=\!CH_2) + CH_2\!=\!C_2H_4$$

Application

Conventional methods used for the identification of different types of PEs are cumbersome and time-consuming. Even IR spectral characterization has not been very successful for LDPE(A) and LDPE(T). The analysis of the variable ethylene quantity produced and the spectral features on five or more CO_2 laser wavelengths are characteristic of each type of PE, which makes this technique a novel noncontact and nondestructive (ND) method for the identification of different PEs. It can be used routinely for both the identification and segregation of different PEs in a mixture. There are a few more important applications of this study which are being evaluated and will be reported in the future, including on-line evaluation of the photostability characteristics of PEs and other polyolefins.

CONCLUSION

This is a unique study in terms of scope and has been possible because of the advantages of sensor technology based on PTBDS which allows real-time spectral analysis of multiple gas species on a ppb level. The results have been analyzed to obtain the following interpretations:

1. Stabilized (commercial) PEs when exposed to low-energy photons (and in the absence of thermal energy) tend to produce ethylene gas without oxidizing the polymers themselves.
2. The mechanism suggested that the ethylene is formed as a result of the above-given rupture of the terminal double bond of the branch chain and not from the main chain of the PE.
3. Quantitative evaluation revealed that the extent of the ethylene gas released is dependent upon the length of branch, that is, the farther the terminal bond is from the main chain, the more ethylene will be released.
4. Apart from the fundamental understanding, this study has also provided one of the most important applications, namely, this is an excellent method for (near) nondestructive and fast identification of different PEs which otherwise involves long multistep cumbersome procedures.

This work was undertaken as a part of collaborative project sponsored by Indo-French Centre for Advance Research, New Delhi. The authors would like to express their sincere thanks to Dr. S. K. Awasthi, GM and head (R&D), IPCL Baroda, for his critical comments and suggestions. The active and fruitful discussions with Dr. Shashikant and Dr. A. B. Mathur of IPCL during the course of preparation of the manuscript is gratefully acknowledged.

REFERENCES

1. C. Vasile, in *Handbook of Polyolefins,* C. Vasile and R. B. Seymore, Eds., Marcel Decker, New York, 1993.
2. B. Zimering, A. C. Boccara, and G. C. Pandey, *Prog. Natl. Sci.,* **6,** S-606 (1996).
3. J. Lacosté, D. J. Carlsson, S. Falicki, and D. M. Wiles, *Polym. Degrad. Stab.,* **34,** 309 (1991).
4. A. Torikai, H. Shirakawa, S. Nagaya, and K. Fueki, *J. Appl. Polym. Sci.,* **40,** 1637 (1990).
5. B. Zimering and A. C. Boccara, *Rev. Sci. Instrum.,* **67,** 1891 (1996).
6. D. Bicanic, A. M. Solyom, G. Z. Angeli, H. Wegh,

M. Posthumus, and H. Jalink, *Infrared Phys. Technol.,* **35,** 637 (1994).
7. P. L. Meyer and M. W. Sigrist, *Rev. Sci. Instrum.,* **61,** 1779 (1990).
8. M. W. Sigrist, *Opt. Eng.,* **34,** 1917 (1995).
9. H. Sauren, D. Bicanic, H. Jalink, and J. Reuss, *J. Appl. Phys.,* **66,** 5085 (1989).
10. F. Harren, J. Reuss, D. Bicanic, and E. Woltering, in *Photoacoustic and Photothermal Processes in Gases,* P. Hess, Ed., Springer-Verlag, Berlin, 1989, p. 148.
11. R. F. Adamowicz and K. P. Koo, *Appl. Opt.,* **17,** 2938 (1979).
12. R. A. Rooth, A. J. L. Verhage, and L. W. Wouters, in *Photoacoustic and Photothermal Phenomena II,* J. C. Murphy, J. W. Maclachlan-Spicer, L. Aamodt, and B. S. H. Royce, Eds., Springer-Verlag, Berlin, Heidelberg, 1990.
13. D. Fournier, A. C. Boccara, N. M. Amer, and R. Gerlach, *Appl. Phys. Lett.,* **37,** 519 (1980).
14. S. Bialkowski and Z. F. He, *Anal. Chem.,* **60,** 2674 (1988).
15. H. DeVries, F. J. M. Harren, G. P. Wyers, R. P. Otjes, J. Slanina, and J. Reuss, *Atm. Envir.,* **10,** 1069 (1995).
16. F. Gugamus, in *Mechanisms of Polymer Degradation and Stabilization,* G. Scott, Ed., Elsevier, New York, 1987, p. 169.
17. F. Gugamus, *Angew. Makromol. Chem.,* **158/159,** 151 (1988).
18. F. Gugamus, *Makromol. Chem. Makromol. Symp.,* **25,** 1 (1989).
19. F. Gugamus, *Macromol. Chem. Makromol. Symp.,* **27,** 25 (1989).
20. F. Gugamus, *Angew. Macromol. Chem.,* **176/177,** 27 (1990).
21. F. Gugamus, *Angew. Macromol. Chem.,* **182,** 85 (1990).
22. F. Gugamus, *Angew. Macromol. Chem.,* **182,** 111 (1990).
23. F. Gugamus, *Polym. Degrad. Stab.,* **27,** 19 (1990).
24. H. Hinsken, S. Moss, J. R. Panguet, and R. H. Zweifel, *Polym. Degrad. Stab.,* **34,** 279 (1991).
25. M. Iring and F. Tudös, *Prog. Polym. Sci.,* **15,** 217 (1990).
26. K. Barabus, M. Iring, T. Kelen, and F. Tudös, *J. Polym. Sci. Polym. Symp.,* **57,** 65 (1976).
27. K. Barabus, M. Iring, S. Laszlo Hedvig, T. Kelen, and F. Tudös, *Eur. Polym. J.,* **14,** 405 (1978).
28. A. Hoff and S. Jacobsson, *J. Appl. Polym. Sci.,* **26,** 3409 (1981).
29. A. Hoff and S. Jacobsson, *J. Appl. Polym. Sci.,* **29,** 465 (1984).
30. G. C. Pandey, B. P. Singh, and A. K. Kulshreshtha, *Polym. Test.,* **9,** 341 (1990).
31. A. K. Kulshreshtha, B. P. Singh, A. V. Panter, and G. C. Pandey, IPCL Internal Report (RD/AAS/MSG/007-68/87), Indian Petrochemicals Corp., Ltd., Baroda, India, 1987.
32. R. Kuhn, H. Kromer, and G. Rossmanilk, *Colloid Polym. Sci.,* **260,** 1083 (1982).
33. A. Dahme and J. Dechant, *Acta Polym.,* **33,** 546 (1982).
34. B. Popli, M. Glotin, and L. Mandelkern, *J. Polym. Sci. Polym. Phys. Ed.,* **22,** 407 (1984).
35. K. W. Doak, consultant, *Ethylene Polymers in EPST,* 1st ed., John Wiley & Sons, New York, Vol. 6, 1980.
36. J. C. Woodbrey and P. Ehrilich, *J. Am. Chem. Soc.,* **85,** 1580 (1963).
37. V. Cornelia and R.-B. Seymour, Eds., *Handbook of Polyolefins,* Marcel Decker, New York, 1993.
38. G. C. Pandey, *Process Control Qual.,* **7,** 173 (1995).
39. G. C. Pandey, S. Sivaram, and Shashikant, IPCL Internal Report (RD/AAS/FTIR-COP/37/88), Indian Petrochemical Corp. Ltd., Baroda, India, 1988.